Monotonic and bimodal size distributions of surface nanowires caused by postdeposition annealing

V. I. Tokar[1,2] and H. Dreyssé[1]

[1]*IPCMS, Université de Strasbourg–CNRS, UMR 7504, 23 rue du Loess, F-67034 Strasbourg, France*

[2]*Institute of Magnetism, NAS and MES of Ukraine, 36-b Vernadsky Boulevard, 03142 Kiev-142, Ukraine*

(Received 26 December 2010; revised manuscript received 29 May 2011; published 31 August 2011)

Reversible growth of one-dimensional monatomic islands (or nanowires) on the steps of vicinal surfaces has been modeled with the use of the rate equations and the kinetic Monte Carlo technique. It has been found that the size distributions of the islands grown during low-temperature deposition quickly change their shape under postdeposition annealing at higher temperature provided the average island size at the high temperature thermal equilibrium is smaller than that corresponding to the low-temperature island size distribution (ISD). This process of antiripening produces in the course of its evolution bimodal and monotonous ISDs with characteristic shapes distinct from the geometric equilibrium ISD. The fast kinetics associated with this process can be used to weaken the influence of competing processes on the kinetics, thus facilitating an accurate determination of the growth parameters. Experimental setups needed for experimental verification of the theoretical predictions are briefly discussed.

DOI: 10.1103/PhysRevB.84.085456 PACS number(s): 81.07.Gf, 68.55.−a, 81.15.Aa

I. INTRODUCTION

The growth of surface nanostructures has been extensively studied in the past years as a prospective tool of nanoengineering.[1] In technological application of major importance are the means of modeling and control. Theoretical simulations, however, are severely hampered by poor knowledge of mechanisms and parameters governing the growth. For example, there is no agreement even on the mechanism of the growth of the atom-thick one-dimensional (1D) surface nanowires, arguably, the simplest of all nanostructures.[2–9]

Much debate caused the monotonically decreasing size distributions of 1D nanowires of group III metals on Si(100) surface studied in Refs. 2 and 5–9. It was noted that such distributions naturally arise at thermal equilibrium[3,4] but in the case of Ga atoms the interatomic interaction found from the fit to experimental data[4] was essentially weaker than that obtained in *ab initio* calculations.[10] At strong interatomic binding, however, the equilibrium cannot be reached under conventional growth conditions, in which case the irreversible growth takes place. However, the latter leads to monomodal island size distributions (ISDs).[11,12] In Refs. 6 and 9 it was suggested that in the irreversible growth the monotonous ISDs may appear as a consequence of nucleation on surface defects. Additional research, however, showed that this mechanism alone is insufficient to quantitatively explain existing data.[7] Therefore, in recent studies some growth reversibility was admitted in the hope that it would contribute to the monotonous behavior.[9,13,14] Furthermore, other mechanisms leading to monotonous ISDs exist, such as nucleation via exchange with the substrate and the adatom evaporation.[15–19] In Ref. 9 it was noted that with several mechanisms leading to qualitatively similar ISDs it is difficult to make a distinction between different models and that additional data are needed to identify the correct growth mode(s). Obviously, it would be desirable to be able to establish the nature of the growth experimentally without resort to theoretical modeling.

In the present paper we discuss a possibility to distinguish the reversible and irreversible growth modes using the postdeposition annealing. We show that in the case when the average size of the islands before the annealing is larger than that after the annealing, the change of the ISD can be very fast. We call this process antiripening because in the absence of the deposition the islands can diminish their average size only when the large islands would mainly evaporate the atoms while small islands would grow at their expense, that is, exactly the opposite to what is taking place during the ripening.

We show that the antiripening can be so fast that it can take place even in the cases where the annealing was not intended or deemed important. For example, sometimes the experimental setup is being used when deposition is carried out at a low temperature while STM images for convenience are taken at a higher temperature (see, e.g., Ref. 20 and references therein). This technique has been developed for strongly irreversible growth when the exposition to higher temperature does not influence the ISD. However, in the case of appreciable reversibility the ISD shape can undergo qualitative change even during a short annealing. In particular, we predict that the growth conditions can be adjusted in such a way that in a 1D system with homogeneous nucleation the ISD can acquire a bimodal form. This finding may be of importance also for the 2D growth where bimodal ISDs were observed experimentally and were explained by the nucleation via exchange with the substrate[21–24] and by excessive misfit strain.[25]

Besides, the high speed of the antiripening kinetics allows for its effects to manifest themselves during short annealing time so the competing slower processes cannot significantly distort the data. It should be remembered that heteroepitaxial structures at the surface are intrinsically unstable because at the true thermal equilibrium they should either dissolve in the bulk or evaporate. Therefore, such slow kinetics as, for example, the Ostwald ripening, cannot be reliable sources of growth parameters because other kinetics, such as intermixing with the substrate or evaporation may significantly obscure other processes. Therefore, the antiripening can be used to measure some parameters of reversible growth with better precision.

We illustrate the above points with the use of the mean-field rate equations and the kinetic Monte Carlo (KMC) technique which we introduce in Sec. III; in Sec. IV we use these

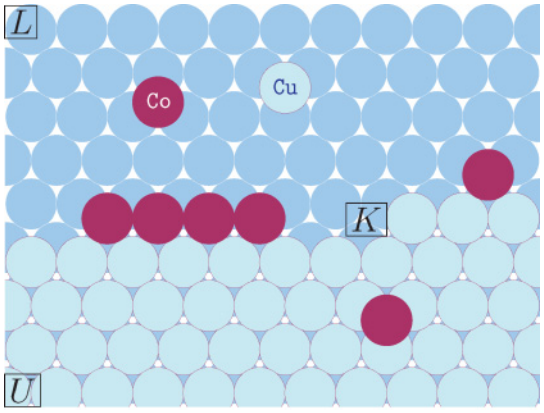

FIG. 1. (Color online) Schematic picture of the deposition of cobalt atoms on a vicinal copper surface. The lower (L) and the upper (U) Cu(111) terraces are separated by a B-type step with a kink (K). Shown are two cobalt and one copper atoms diffusing on the terraces, as well as a four-atom cobalt island and a single cobalt atom attached to the step. (For further explanations, see the text.)

techniques to simulate the growth of 1D nanowires using as an example the monatomic Co wires on the steps of the Cu(775) vicinal surface studied in Ref. 20; this system is briefly discussed in Sec. II. In the concluding Sec. V we discuss some experimental consequences of our predictions.

II. 1D GROWTH ON THE STEPS OF A VICINAL SURFACE

Heteroepitaxial growth is a complex phenomenon whose theoretical modeling requires knowledge of a large number of parameters which describe numerous kinetic processes underlying the growth. Because of their simple geometry, the number of parameters is considerably reduced in the case of 1D nanostructures.[2,5–9] From a theoretical point of view the simplest systems are those that can be adequately represented by purely 1D models because in many cases such models can be solved exactly, which makes their analysis particularly easy.[3,20,26–28] However, care needs to be taken in the application of such models to real systems because real physical objects are always 3D. The 1D modeling is usually based on some assumptions whose validity needs to be justified. Because there exist many possibilities for embedding 1D structures into 3D systems, for concreteness we discuss the problems that arise here using as an example the Co/Cu(775) system studied in Ref. 20.

The growth in this system is shown schematically in Fig. 1. As can be seen, the step with kinks can be formally viewed as a stepped 1D "surface" with the kinks playing the role of the zero-dimensional "steps." The steps are mobile due to the copper atoms diffusing on the terraces which can attach and detach to/from the kinks. In the experimental data of Ref. 20 the kink mobility at room temperature (RT) was seen as the frizz on the STM photographs, which means that the mobility of the kinks at RT was high.

If for the time being we forget about the kinks, the growth on the steps proceeds as follows. The cobalt atom arrives on the surface and diffuses on a terrace until attaching to the bottom of a step edge, where it creates either a mobile monomer on the 1D surface or an end atom of an island (see Fig. 1). Such purely 1D kinetics were observed in this system at low coverages $\theta \lesssim 0.1$, where the islands remained strictly 1D; that is, no second-row nucleation was seen. In an exhaustive theory this behavior should have been explained but in the model of Ref. 20 it was accepted as an empirical fact.

Even more drastic simplification is achieved if the state of thermodynamic equilibrium is assumed. This is because the equilibrium state is unique and does not depend on the kinetics which led to it, so the kinetic parameters can be ignored. Thus, the system can be fully characterized by the Hamiltonian which in the case under consideration can be chosen in the form of a lattice gas model with nearest-neighbor (NN) interactions between the atoms (explicit *ab initio* calculations[29] show that the NN interactions between Co atoms on the Cu surface dominate),

$$H_{NN} = -\epsilon_2 \sum_i n_i n_{i+1}, \tag{1}$$

where ϵ_2 is the strength of the NN interatomic interaction, $n_i = 0, 1$ describes the occupation of site i by an adsorbed atom, and index i numbers the deposition sites along the step edge. The deposition site is defined as the energetically favorable place of attachment of the adsorbed atom to the step (see Fig. 1). The deposition is considered to be coherent because of small size misfit between the cobalt and copper atoms.[30]

As is known, with the use of the substitution $n_i = (s_i + 1)/2$, where $s_i = \pm 1$, the lattice gas model can be transformed into the Ising model whose exact solution in the 1D NN case is well known. Equilibrium ISDs for heteroepitaxial systems described by Hamiltonian Eq. (1) were calculated in Refs. 26 and 3 and used in Ref. 20 to fit experimental data on the Co/Cu(775) heteroepitaxy. The fit at coverage $\theta = 0.09$ made it possible to assess the interaction parameter $\epsilon_2 \approx 0.13$ eV.

This, however, is almost an order of magnitude smaller than the value 1.2 eV of the NN interaction between two Co atoms placed on the Cu(111) substrate found in *ab initio* calculations of Ref. 29. One may argue that $\epsilon_2 = 0.13$ eV corresponds to the Co atoms attached to the step. However, it is hardly possible that in the vicinity of a step the interatomic interaction would diminish almost ten times. For example, the difference in the binding energies between the isolated Co dimer[31] and the dimer placed on the Cu(111) surface[29] is at most 25%. This situation is similar to the heteroepitaxy of the gallium atoms on silicium surface mentioned in the Introduction.[2] Because the interaction parameter found from the fit to an equilibrium distribution turned out to be several times smaller than in *ab initio* calculations,[4,10] an alternative explanation of the monotonous ISDs was proposed based on the nucleation on surface defects.[6,9]

However, in the Co/Cu(775) system there also exists a possibility of nucleation on the defects, namely, on the kinks which should be preferable places for island nucleation because of the higher coordination they provide for the adsorbed atoms (see Fig. 1). It is remarkable that the kinks share with the C-type defects of Refs. 6 and 9 the property that the island grows only on one side of the defect. Thus, similar to the above references, the kinks could be responsible for monotonous ISDs provided their concentration was sufficiently high for the majority of islands to nucleate on them.[14]

In Ref. 32 the kink formation energy was found to be $E_K \approx 0.116$ eV so the *equilibrium* concentration of these 1D steps directed on both sides is

$$c_K \approx 2e^{-E_K/k_BT}. \quad (2)$$

According to this formula, at the RT c_K is about 2%, which is more than enough for all islands to be nucleated on the kinks because the island concentration $N = \theta/s_{av} \approx 0.1/30 \approx 0.3\%$. However, the deposition was carried out at $T = 165$ K. At this temperature the equilibrium concentration $c_K \approx 0.06\%$, which is five times less than the number of islands. To resolve this difficulty additional information on the thermal history of the experimental specimens would be helpful. Most probably, the specimens started their evolution at RT, where $c_K \approx 2\%$. Then they were cooled down to 165 K for the deposition. The information which would be necessary is how long the specimens were annealed at this temperature before the start of the deposition. A kinked surface step can be formally considered as an assembly of $1 + 1$D islands on a flat substrate (assuming for simplicity that the 1D surface represented by the step is not vicinal). As temperature goes to zero, the islands should flatten to reduce the kink concentration. This process can be rather slow because of slow kinetics at low temperature so the kink concentration at which the cobalt deposition had taken place could be sufficient to nucleate the majority of islands. However, to simulate this scenario we would need a detailed thermal history of the ingot before the deposition which is missing.

It should be noted, however, that in contrast to C-type defects whose surface concentration did not change during the deposition,[6,9] the number of kinks is not conserved. So there is another possibility for the nucleation. When some or all of the kinks are "passivated" by attached cobalt atoms, the equilibrium between the copper-terminated kinks and the copper atoms on the terraces (the $1 + 1$D "vapor" atoms—see Fig. 1) will be violated, so new kinks should appear. This may provide the necessary number of kinks for the majority of islands to be nucleated in this way. This may serve as a mechanism of island nucleation with the critical nucleus size equal to zero.[11,16,18,33,34] This case is characterized by monotonous[11,16,18,33,34] or bimodal ISDs.[23,35,36] Another possibility of realization of the nucleation of this type is the exchange of the adsorbate atoms with the substrate.[16,23,34–36] The latter process was observed experimentally in Ref. 20 [see their Fig. 2(d)]. It should be noted that only the exchange in the immediate vicinity of the step edge or within the edge itself will nucleate 1D islands we are discussing.

Yet another mechanism of monotonous ISD formation is the adsorbate evaporation.[17,18] In our $1 + 1$D model three evaporation mechanisms are possible: The evaporation from the substrate into the surrounding space of the camera, detachment of atoms from the step edge and subsequent exchange with the substrate atom, and the dissolution of adatoms on the steps into the substrate bulk.

Besides, in Sec. IV we study the antiripening mechanism of the growth leading to monotonous and bimodal ISDs which only partly exploits the reversibility and thus can be operative when the interatomic binding is not strong enough to produce completely irreversible growth, yet it is sufficiently strong for the complete thermal equilibration to be impossible on the experimental time frame.

III. SIMULATION TECHNIQUES

As was noted in the Introduction, the difficulties with predictable modeling of heteroepitaxial growth to a large degree are a consequence of our poor knowledge of the growth parameters. This is because currently they cannot be reliably measured or calculated separately but should be found from a fit of the growth model to experimental data (see, e.g., Refs. 2, 20, 37 and 14). Therefore, numerically accurate growth modeling is very important.

The most popular tool in the growth simulations is the KMC technique because given a model it provides, in principle, its exact solution. A serious drawback of the KMC, however, is that it is very computationally demanding when good statistics are needed. Taking into account that the experimental data are rather noisy, the interpretation of the simulations is not always convincing and the fitted parameters cannot be defined with sufficient accuracy.[14,19] Because of this, of great interest are exact analytical solutions which can be obtained in 1D case at equilibrium[3,20,26–28] and also the rate equations which usually can be improved so as to provide very good agreement with the exact KMC data.[12,38]

For simplicity, in our simulations in the next section we explicitly treat only the case described by Hamiltonian Eq. (1). This model is considered to be adequate for the Co/Cu(775) system studied in Ref. 20, which we use as a concrete example of nanowire growth. The Co/Cu system was also studied in Refs. 29 and 37 and it was found that the NN interactions dominate[29] and that the size misfit between the substrate and the deposit is small.[37]

In heteroepitaxial systems, however, negligible misfit is an exception rather than the rule. Therefore, the general formalisms we discuss below are suitable to account for the misfit in the harmonic approximation.[27,28] In Refs. 27 and 28 it was shown that a system with only NN "chemical" interaction and the misfit strain can be described by a cluster generalization of Hamiltonian Eq. (1), where all interactions are confined to the contiguous sequences of atoms as

$$H = -\sum_i (\epsilon_2 n_i n_{i+1} + \epsilon_3 n_i n_{i+1} n_{i+2} + \cdots), \quad (3)$$

where ϵ_2, ϵ_3, . . ., are the interactions within the clusters of two, three, etc., adjacent atoms. As is seen, if two islands are separated by at least one vacant site all interactions in Eq. (3) containing this site become zero. Such interactions appear in epitaxial systems with size misfit and can lead to the island size calibration.[27,28,39]

A. Thermal equilibrium

In the conventional notation of the growth theory[11,12,33] the exact expression for the ISD of the model defined by Eq. (3) derived in Refs. 27 and 28 reads

$$N_s^{(eq)} = (1 - \theta - N) \exp[(\mu s - E_s)/k_BT], \quad (4)$$

where N_s is the per site density of the islands of size s, the coverage θ is equal to the total number of atoms M divided by L, the number of the deposition sites in the system,

$$N = \sum_{s=1}^{L} N_s, \tag{5}$$

is the total island density, μ is the chemical potential-like parameter which fixes the total number (M) of the deposited atoms (i.e., the coverage), and E_s is the energy of an island of size s calculated with the use of Eq. (3). The meaning of the first coefficient in Eq. (4) is easy to understand by multiplying the whole expression by the total length of the system L. Now this coefficient became $L - M - K$, where $K \equiv LN$ is the total number of islands. Thus, the number of islands of size s $M_s = LN_s$ is proportional to the statistical weight given by the exponential factor and to the available free phase space. The latter is given by the number of empty sites $L - M$ available for the deposition minus one empty site per each island (hence, K sites in total) because if an island of size s were placed near another island without an empty space between them, then a new island corresponding to larger size would form while the island of size s would disappear.

In the absence of the strain contributions the Hamiltonian Eq. (3) reduces to Eq. (1), where only the "chemical" interaction ϵ_2 is present. The energy of the island of size s in this case is

$$E_s = -\epsilon_2(s-1), \tag{6}$$

so Eq. (4) can be cast in the form

$$N_s^{(eq)} = (1 - \theta - N)e^{-Q}p^s, \tag{7}$$

where

$$Q = \epsilon_2/k_BT \tag{8}$$

and $p = \exp[(\mu + \epsilon_2)/k_BT]$. In this notation in the thermodynamic limit $L \to \infty$,

$$N = \sum_{s=1}^{\infty} N_s = (1 - \theta - N)e^{-Q}p/(1-p). \tag{9}$$

Here and below we omit the superscript (eq) because the definitions of N and θ are valid also in general case. The coverage can be calculated from Eq. (9) by applying $p(d/dp)$ to the right-hand side:

$$\theta = \sum_{s=1}^{\infty} sN_s = (1 - \theta - N)e^{-Q}p/(1-p)^2. \tag{10}$$

Now dividing Eq. (9) by Eq. (10), one gets

$$p = 1 - N/\theta. \tag{11}$$

This can be substituted back to Eq. (9) to give

$$e^Q = (1 - \theta - N)(\theta - N)/N^2. \tag{12}$$

In the equations above all densities can be expressed through the experimentally measurable numbers L, M, and K. In this case the ISD and the interaction parameter ϵ_2 can be expressed through the observable quantities and we thus recover the formulas of Refs. 3, 20 and 26. We note, however, that the experimental numbers of this type do not have much physical meaning because they depend on the size of the specimen studied. More physical formulas can be obtained by expressing the right-hand side of Eqs. (11) and (12) in terms of the average island size[4]:

$$s_{av} = \theta/N. \tag{13}$$

Now we can express the left-hand side of Eq. (12) as

$$e^Q = (1 - \theta - \theta/s_{av})s_{av}(s_{av} - 1)/\theta \tag{14}$$

and derive the exact expression for the average island size,

$$s_{av} = \frac{1/2}{1-\theta} + \sqrt{\frac{\theta e^Q}{1-\theta} + \left(\frac{1/2-\theta}{1-\theta}\right)^2}. \tag{15}$$

Equations (14) and (15) relate the interaction parameter ϵ_2 (via Q) with the intensive quantities s_{av}, θ, and T.

B. Rate equations

In the studies of irreversible growth it was found that the mean-field rate equations can be improved in such a way as to give very accurate solutions,[11,12,33] thus providing a viable alternative to computationally intensive KMC simulations. Generalization of the mean-field equations to the reversible growth is completely straightforward.[38] It is not evident, however, that non-mean-field corrections derived for irreversible growth can be successfully used also in this case.

In the present paper we show that the detailed balance condition combined with the island density-dependent capture numbers introduced in Ref. 12 for irreversible case make it possible to describe the reversible case in a semiquantitative manner both with and without the deposition flux and across many orders of magnitude of the time scale.

The mean-field rate equations (5) and (6) of Ref. 38 for the reversible growth can be cast in the form

$$\frac{dN_1}{dt} = F + 2\Delta_2 + \sum_{s>2} \Delta_s, \tag{16a}$$

$$\frac{dN_s}{dt} = \Delta_{s+1} - \Delta_s, \quad s > 1, \tag{16b}$$

where

$$\Delta_s = K_s^- N_s - K_{s-1}^+ N_1 N_{s-1}, \tag{17}$$

F is the deposition flux, and $K_s^{\pm}$ are the kernels describing either capture (+) or detachment (−) of monomers by or from the islands of size s. The capture kernel is defined as

$$K_s^+ = D\sigma_s, \tag{18}$$

where D is the monomer diffusion constant and σ_s the capture number.[11,33] The detailed balance condition requires that

$$K_s^- = K_{s-1}^+ \exp(\Delta E_s/k_BT), \tag{19}$$

where $\Delta E_s = E_s - E_{s-1}$. The formalism is quite general and can be used for simulating growth in any number of dimensions. The capture numbers from Ref. 12 which we will use in our simulations are specific to 1D systems:

$$\sigma_1 = 4[(2-\beta)N_1 + \beta N], \tag{20a}$$

$$\sigma_{s>1} = \beta\sigma_1, \tag{20b}$$

where the coefficient $\beta = 1.389$ accounts for some non-mean-field features (the mean-field value of β is unity). Formal difference of Eq. (20a) from the expression of Ref. 12 is because of our definition of the total island density in Eq. (5) which includes the monomers ($s = 1$) in contrast to the definition of N in Ref. 12.

It is easy to see that the expression derived from the law of mass action in Ref. 40,

$$N_s^{(eq)} \simeq \exp[(\mu s - E_s)/k_B T], \tag{21}$$

satisfies

$$\Delta_s = 0.$$

Hence, the ISD Eq. (21) is the equilibrium distribution because it satisfies the stationary Eqs. (16) in the absence of the deposition flux ($F = 0$). Equation (21) approximates the exact 1D distribution Eq. (4) at low coverages $\theta \ll 1$ (we remember that $N = \theta/s_{av}$). This defines the range of validity of the rate equations (16).

IV. GROWTH KINETICS

Our aim in the present paper is to study annealing behavior in 1D heteroepitaxial systems with sufficiently strong reversibility. By the latter we mean such reversibility that is easily detectable under conventional experimental setups. In particular, such systems should exhibit strong tendency to equilibration. In the 1D case this will show itself in the ISD close to the geometric distribution Eq. (7) because usually the NN interaction dominates. Our major simulation tool is the KMC technique, which gives practically an exact solution to the model studied. The conventional activated hopping dynamics is used.[41] Our model is a straightforward extension of the irreversible 1D system we studied in Ref. 42. For simplicity, only the detachment of atoms from the island ends was taken into account while the interior atoms were considered to be inactive due to their stronger binding. The KMC technique, however, is computationally rather demanding. In the simulations below we used the system consisting of $L = 2^{18} \approx 2.6 \times 10^5$ deposition sites and the statistics were gathered from 20–40 parallel processes. Still, as is seen below, the data obtained are rather noisy. Therefore, we duplicated the simulations with solutions of the rate equations. To establish the contact between the two approaches the formula for the diffusion constant in terms of the hopping rates was used:

$$D = \frac{\nu}{2} e^{-E_e/k_B T}, \tag{22}$$

where ν is the attempt frequency (in Ref. 37 assessed to be equal to 10^{12} in the Co/Cu system) and E_e is the activation energy for the edge diffusion.

Though the techniques we use are fully general, below for concreteness we use explicit parameters corresponding to the growth of the Co wires on the steps of a vicinal copper surface, which was studied, in particular, in Refs. 20 and 37. In this study statistical data were gathered for two 1D, coverages $\theta = 0.09$ and $\theta = 0.12$, so below for simplicity we consider only one coverage $\theta = 0.1$.

The value of interatomic coupling found in Ref. 20 was $\epsilon_2 = 0.13$ eV. Co was deposited at 165 K during ~10 min and the STM measurements carried out at the RT revealed approximately geometric (exponential) ISDs with average island sizes $s_{av} \approx 27$ and $s_{av} \approx 40$ atoms at coverages $\theta = 0.09$ and $\theta = 0.12$, respectively. According to Eq. (15) at coverage 0.1 the equilibrium value at 165 K $s_{av} \approx 33$.

According to Ref. 37 the activation energy of diffusion along the step edges $E_e = 0.35$ eV, so the ratio $R = D/F$ of the diffusion constant Eq. (22) to the deposition flux $F = 0.01$ ML/min can be calculated as $R \approx 6 \times 10^4$. In the irreversible growth theory this is considered to be a rather low value, which means that the deposition is fast.[11,12,33] Therefore, we may neglect the reversibility and assess the average island size with the use of the asymptotic formula,[11]

$$s_{av} \sim (2\theta^3 R/\pi)^{1/4}, \tag{23}$$

which gives $s_{av} \sim 2.5$ atoms, that is, a value which is much smaller than the needed 33 atoms estimated above. This situation only slightly improves if exact KMC simulations and the reversibility are taken into account: $s_{av} \simeq 4$ (see Sec. IV A below).

Thus, the mobility of atoms at 165 K as assessed above is too small to equilibrate the system. To understand whether the equilibrium or, at least, a monotonous ISD can be obtained in this system during deposition at 165 K we carried out both KMC and the rate equations simulations with the value of $R = 6 \times 10^8$ or four orders of magnitude larger than that calculated on the basis of the data of Ref. 37. This corresponds to assuming that the diffusion barrier is ~30% less than 0.35 eV, that is, $E_e = 0.22$ eV. This is still larger than the barrier for the surface diffusion $E_{surf} = 0.19$ eV, so some influence of the larger coordination at the step edge is taken into account. We note in passing that the edge diffusion can be faster than the surface diffusion (see Ref. 43 and references therein) so even larger values of R are, in principle possible. From a more general standpoint, because of the Arrhenius dependence in Eq. (22), the diffusion constant is very sensitive to small errors in both calculations and in experiment. So, in practice, D is often used as a fitting parameter.[44] Thus, our choice of another value of D can be viewed as an attempt to fit the model to experimental data.

The results of the simulations both with the use of the rate equations and with the KMC are presented in Fig. 2. From the simulation data we see that at the end of the deposition the ISD is monotonous but with some negative curvature of the logarithm of the island density [the logarithm of the equilibrium distribution Eq. (4) should be a straight line]. However, experimental data, especially at coverage $\theta = 0.12$ shown in the inset, are also far from being a straight line. (The first point in the inset is placed at $s = 7$ because the island statistics in Ref. 20 were gathered in the bins of size ~12: $s = 1$–12, 13–25, etc.) Their qualitative behavior, however, is quite different from that of the $t = t_d$ curve. However, as is seen from Fig. 2, under annealing the shape of the ISD begins to qualitatively resemble the experimental curve. Unfortunately, it is hardly possible to explain the experimental data by higher diffusivity and subsequent annealing because of the very fast equilibration kinetics.

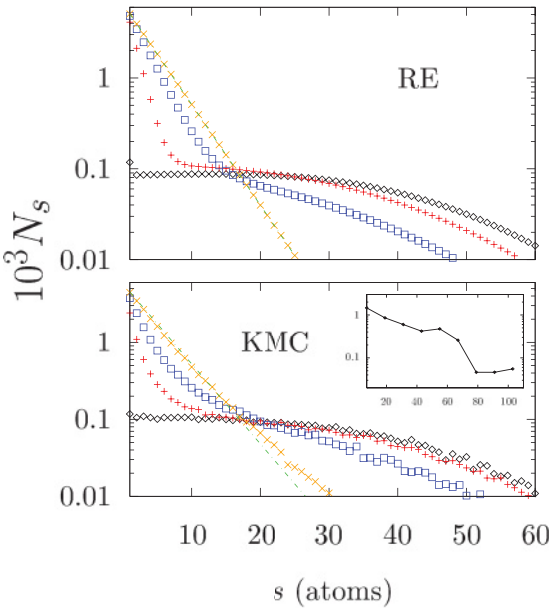

FIG. 2. (Color online) ISDs at the end of the deposition at time $t_d = \theta/F$ ($\diamond$) and after subsequent annealing during $2.5 \times 10^{-4} t_d$ (+), $10^{-3} t_d$ ($\square$), and $10^{-2} t_d$ ($\times$); time is measured in KMC units (the inverse hopping rate of a monomer). The rate equations and KMC simulations data are shown on the upper and the lower panels, respectively. The straight lines correspond to the equilibrium geometric distributions Eqs. (7) and (21) describing, respectively, the KMC and the RE cases. Coverage $\theta = 0.1$ and $\epsilon_2 = 0.13$ eV were chosen to allow qualitative comparison with experimental data of Ref. 20; the ISD corresponding to $\theta = 0.12$ from this reference is shown in the inset. With $R = 6 \times 10^8$ the ISD at the end of deposition was monotonous and $s_{av}^{KMC}(t_d) \approx 24$.

Because the value of the diffusion activation energy E_e is not known with sufficient precision, time t_d in Fig. 2 and in all figures below is measured in the KMC units (the inverse hopping rate of an isolated atom along the step edge). However, we know that the deposition took 10 min. So with the annealing times being given in units of t_d, the corresponding physical time can be found with the use of the coefficient

$$C = \exp\left[\frac{E_e}{k_B}\left(\frac{1}{T_a} - \frac{1}{T_d}\right)\right], \tag{24}$$

which describes the ratio of the KMC time units at the two temperatures: that at the deposition (T_d) and that at the annealing (T_a). With the use of this formulas with $E_e = 0.22$ eV and $T_a = 300$ K (the RT) we find that the annealing time scale in Fig. 2 is very short and corresponds to ~0.1–5 ms. This kinetics can hardly be detected without the use of some sophisticated experimental techniques. In the usual experimental setup only the final equilibrium ISDs shown in Fig. 2 as straight lines are seen with the average island size according to Eq. (15) $s_{av} \approx 4.7$ atoms. Thus, with the measurements carried out at RT the interatomic interaction $\epsilon_2 = 0.13$ is too weak to reproduce the experimentally observed ISDs.

We note that this fast reduction in the average island size can be used as a mean to detect and quantify the reversibility by measuring s_{av} at both low and high temperatures. This kinetics can be useful in effectively reducing the influence of many slow high-temperature processes, thus effectively improving the accuracy of the measurements.

A. 1D coarsening

In a previous section we saw that the equilibration at $T_d = 165$ K is not easy to reconcile with the experimental setup and with the parameters taken from literature sources. Therefore, if we still assume that the ISDs observed were measured at thermal equilibrium, the latter should correspond to $T_a \simeq 300$ K. However, because the experimental values of the average island sizes and the coverages are the same, the NN interatomic interaction ϵ_2 should be equal according to Eqs. (8) and (14) to $0.13(T_a/T_d) = 0.236$ eV. Now, once again assuming the slow diffusion at the deposition temperature and $R = 6 \times 10^4$, we expect that the small islands ($s_{av} \simeq 4$ atoms—see Fig. 3) grown at low temperature will coarsen during annealing to produce large islands distributed according to the geometric law.

As is known, however, at finite temperature there is no different phases in 1D so the conventional phase separation is impossible. One may speak only about some saturated growth. The growth mechanism also is different from the conventional Ostwald ripening. In the latter, the driving force of the growth is the higher atomic pressure near the islands with higher surface curvature (the Gibbs-Thomson effect) which forces the atoms to evaporate from smaller islands and attach to the larger ones. However, this mechanism is inoperative in 1D because all island "surfaces" are the same. Presumably, in 1D the coarsening is driven by the stochastic ripening mechanism proposed in Ref. 45. The mechanism acts as follows: Different islands exchange atoms which they randomly lose or attach. Because of the randomness, occasionally some islands will

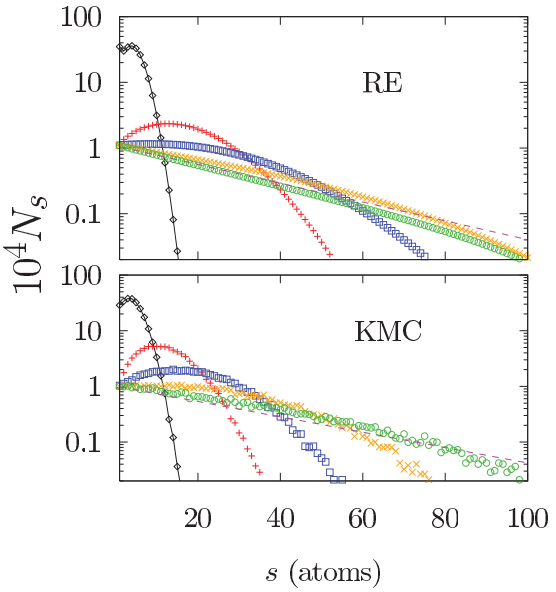

FIG. 3. (Color online) Same as in Fig. 2 but for $R = 6 \times 10^4$ and $\epsilon_2 = 0.236$; the monomodal distribution at the end of the deposition ($\diamond$, the line is guide to the eye) had $s_{av}^{KMC}(t_d) \approx 4$. The ISDs during postdeposition annealing are shown at times $2.5 \times 10^3 t_d$ (+), $10^4 t_d$ ($\square$), $4 \times 10^4 t_d$ ($\times$), and $2 \times 10^5 t_d$ ($\circ$). (All times are measured in KMC time units.)

lose all their atoms and disappear. In this way the average island size in the ensemble will grow because the nucleation is strongly suppressed at low temperature where the monomer concentration is low while it takes at least two atoms to nucleate an island. Because the detachment probability is assumed to be small and the same for wires of any length, the probability for a wire to lose all atoms diminishes exponentially with its size.

This picture is confirmed by our simulations where we saw very slow coarsening with the equilibration time being $\gtrsim 2 \times 10^5 t_d$ in KMC units. Because of the high adatom mobility at the RT, the corresponding time in physical units was not very large. Yet even with $E_e = 0.35$ eV[37] the annealing time $\gtrsim$30 min is necessary according to Eq. (24) to reach a monotonous ISD. This choice of the duration of annealing was motivated by the fact that it approximately corresponds to the time interval the experimental assembly was kept at the RT before the STM photographs were taken.[46] It would be highly desirable to know the temperature history of the specimens during this process since it is quite plausible that they were not subject to the RT during all 30 min because of the finite heating rate of the assembly. However, at small annealing times the ISDs are monomodal, as is seen from the simulated ISDs shown in Fig. 3.

It should also be noted that after 30 min of annealing the ISD is not yet at perfect equilibrium and if the interatomic interaction is considerably stronger than $\epsilon_2 \approx 0.24$, as the *ab initio* calculations suggest,[29] the coarsening scenario of the present section also can hardly be reconciled with all available information.

It is pertinent to note that, experimentally, the time evolution of the ripening ISDs of 1D islands was observed in In/Si system in Ref. 8.

B. Annealing-induced bimodal ISDs

The last scenario we consider is realized when both the enhanced diffusivity ($E_e = 0.22$ eV, $R = 6 \times 10^8$) and stronger binding ($\epsilon_2 = 0.236$ eV) are effective. In this case the shape of the ISD at the end of the deposition is monomodal (see Fig. 4). The difference with the case shown in Fig. 2 is due to stronger interatomic coupling. Similar to that case is the fast annealing to the monotonous ISD. The coefficient C in Eq. (24) in this case is $\sim 10^3$ so the annealing to the monotonous ISD takes about 4 s. In the course of the kinetics the ISD acquires a transient bimodal shape, which can be used for qualitative identification of the antiripening. It should be remembered, however, that similar shapes of the ISDs were observed in the 2D growth and were explained by the nucleation via exchange with the substrate[21–24] and by excessive misfit strain.[25] Careful investigation of possible mechanisms of appearance of bimodal distributions may turn out to be of interest for the interpretation of the Co/Cu(775) data if the bimodal distribution seen in the ISDs at both coverages studied in Ref. 20 (see their Fig. 3) will turn out to be real and not caused by insufficient statistics, as the authors seem to suggest.

Qualitatively, the antiripening mechanism can be explained as follows. When the average island size of the epitaxial islands exceeds the average island size corresponding to equilibrium

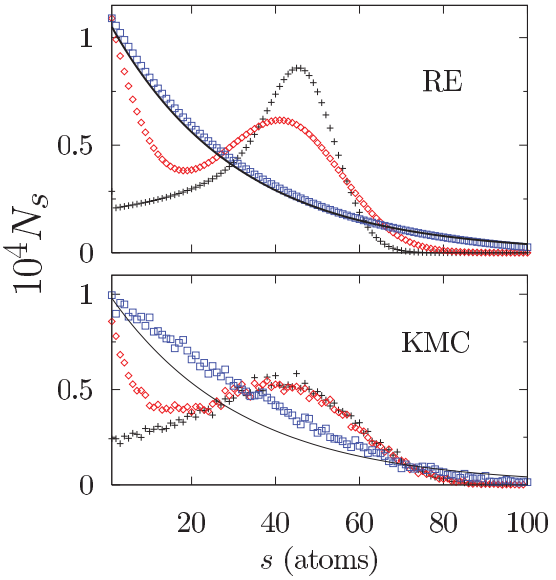

FIG. 4. (Color online) Same as in Fig. 3 for $R = 6 \times 10^8$ (note nonlogarithmic ordinate). Shown are ISDs at t_d (+) and for postdeposition annealing during $0.3t_d$ (◇) and $8.5t_d$ (□); $s_{av}^{KMC}(t_d) \approx 37$. The equilibrium distributions are shown by solid lines.

at the temperature of the substrate, under the annealing the majority of islands will lose atoms to reduce their size. The free monomers thus produced will nucleate small islands which, in contrast to large islands, should grow to attain the equilibrium size. Thus, during some stage of the evolution there will be two distinct distributions: one corresponding to the shrinking large islands and another one which would describe the growing newly nucleated islands. It should be noted that the low-temperature large-size ISD can be both equilibrium and nonequilibrium: The mechanism described will be operative in both cases. The only difference is that when both equilibrium distributions are of geometric character (we recall that this is characteristic for nonstrained systems), the intermediate bimodal distributions will not be observed.

V. DISCUSSION

In the present paper we discussed the problem of formation of monotonous ISDs in heteroepitaxial growth on the surface steps. In particular, we studied the possibility of their explanation by equilibrium statistics as suggested in Ref. 20. The main difficulty with such an explanation is that the strength of the coupling between the cobalt atoms $\epsilon_2 = 0.13$ eV obtained in Ref. 20 from the fit to experimental data is an order of magnitude smaller than the value 1.2 eV found in *ab initio* calculations for the interaction of two NN Co atoms on the Cu(111) substrate.[29] It should be noted that in the STM photographs of Ref. 20 there exists an indirect experimental evidence for larger than 0.13 eV value of ϵ_2. According to Ref. 32, the kink formation energy has about the same value $E_K \sim 0.12$ eV and because this energy corresponds to cutting one copper bond, if the interaction between the cobalt atoms were of similar value then the frizz on the cobalt-decorated parts of the steps would have been comparable to the pronounced frizz observed on the

copper-terminated parts of the steps. Experimentally, however, the cobalt chains are perfectly straight within the resolution of the STM photographs[20] which may indicate that the cobalt bonds are much stronger than the copper ones.

In our study we somewhat alleviated the discrepancy between the fitted and the calculated values of the interatomic bonding by showing that under the hypothesis of thermal equilibrium the experimental data can be fitted to the value of $\epsilon_2 \approx 0.24$ eV, which is about two times larger than 0.13 eV. Still the difference with the *ab initio* estimate remains very large. Some further improvement may be achieved if we assume that the experimental data correspond not to thermal equilibrium but to some intermediate stage of the growth corresponding, for example, to our Fig. 4, where the bimodal ISDs exhibit behavior similar to that seen in both ISDs of Ref. 20. (We recall the data shown on these figures were gathered in the bins of size 12, so the curves are smeared and in reality their bimodal structure should be more pronounced.)

The origin of the bimodal behavior of the curves in Fig. 4 is easily understood: At higher values of island sizes we see the universal scaling curve of the irreversible growth[12] formed during the deposition at 165 K (see the first KMC curve in Fig. 4). At this temperature the value of interatomic binding $\epsilon_2 \approx 0.24$ eV is strong enough for the growth to be irreversible. The same distribution would have been obtained for any value of $\epsilon_2 > 0.24$ eV. In contrast, the first maximum at the bimodal curve in Fig. 4 is fully due to the growth reversibility because it corresponds to the small islands which nucleated from the atoms detached at the RT. The number of such atoms is proportional to the detachment rate which in the simulations shown at the figure corresponds to $\epsilon_2 \approx 0.24$ eV while the annealing lasted about 0.14 s. An elementary estimate shows that during $\sim$30 min of the annealing accomplished in the experiments on the Co/Cu(775) growth,[46] a similar quantity of atoms could have been evaporated with the detachment rate corresponding to $\epsilon_2 \approx 0.34$ eV at most. Presumably, this is the maximum value which can be reconciled with the assumption of the growth reversibility in the experiments of Ref. 20 because if the bimodal character of the data is indeed statistically insignificant and the true ISDs are monotonous, then the experimental data would be described by the curves in Fig. 4 corresponding to later stages of annealing which would require smaller values of ϵ_2 in order for the ISD shape to be reached during $\sim$30 min.

The value $\epsilon_2 \approx 0.34$ eV, however, is still considerably smaller than the *ab initio* estimate.[29] To resolve this controversy experimentally we propose to exploit the antiripening growth mode. The peculiarity of the antiripening kinetics which distinguishes it from other growth modes is that it leads to diminution of the average island size of the ISD in the absence of the deposition flux. Obviously, this is possible only if the detachment of atoms from islands takes place, so the antiripening can be used to detect and quantify the strength of the interatomic coupling. Experimental realization of this phenomenon may require annealing at rather high temperature, where many other processes became energetically allowed. The fastness of the antiripening kinetics, however, can be helpful in separating it from the competing processes.

Though only 1D systems were explicitly treated in the present paper, the simple physics underlying the antiripening should be operative also in higher dimensions. Critical to the reversibility is the possibility of the atomic detachment which presupposes sufficiently weak interatomic interaction. Some systems with monolayer-high 2D islands and sufficiently weak interatomic coupling are listed in Part II of Ref. 33. The evaporation from 2D islands was already observed in Ref. 47 in the ripening regime. As is known, the ISD at ripening acquires a monomodal shape.[48,49] However, it is quite obvious that the heating above the phase separation temperature will, on the one hand, enhance the evaporation; on the other hand, the system will strive to reach a monotonous ISD (some distributions of 2D islands observed in Ref. 21 are quite close to being monotonous). Thus, at intermediate stages a bimodal distribution should be observable.

Experimental realization of the antiripening should not be very difficult. Having chosen some high temperature where the average island size is sufficiently small it is necessary to choose a not-too-low temperature and to adjust the deposition flux in such a way that the ensuing ISD is monomodal and has the average island size larger than the higher-temperature one. In this way bimodal distribution at intermediate annealing stages should be seen. It must be remembered, however, that there exist competing processes that were mentioned in the Introduction which may lead to bimodal distributions and which were invoked to explain the bimodal ISDs observed in 2D growth in Refs. 21–24.

The bimodal ISDs should be easier to detect because their shape is qualitatively different from both the monomodal ISDs due to the irreversible growth at low temperature and from the monotonous equilibrium ISDs. However, the antiripening of monotonous ISDs (see Figs. 2 and 4) should be easier to realize experimentally by simply equilibrating the system at some temperature and then annealing it at a higher temperature.

To conclude, in the present paper, with the use of the the rate equations and the KMC simulations, we investigated the reversible growth of 1D epitaxial islands. We studied possible scenarios of postdeposition annealing and showed that it may produce nonequilibrium monotonous and bimodal ISDs. The antiripening kinetics found in our simulations can be used to identify the reversible growth and assess the kinetic parameters.

Because the growth of surface nanostructures is a technologically important process, there exists a need in the tools for its predictive simulation. The use of the KMC method is not practical because of the necessity to gather voluminous statistics. As a byproduct of our study, we showed that good semiqualitative description of the reversible growth can be achieved with the use of the rate equations corrected for non-mean-field behavior. We included only the simplest correction derived in Ref. 12. However, in the case of irreversible growth it was possible to further improve the equations to such a degree as to reach almost perfect agreement with the KMC.[12] This gives hope that similar improvement can be achieved also in the reversible case.

ACKNOWLEDGMENTS

The authors acknowledge CNRS for support of their collaboration. One of the authors (V.I.T.) expresses his gratitude to Université de Strasbourg and IPCMS for their hospitality.

[1]J. V. Barth, G. Costantini, and K. Kern, Nature (London) **437**, 671 (2005).
[2]M. A. Albao, M. M. R. Evans, J. Nogami, D. Zorn, M. S. Gordon, and J. W. Evans, Phys. Rev. B **72**, 035426 (2005).
[3]P. Gambardella, H. Brune, K. Kern, and V. I. Marchenko, Phys. Rev. B **73**, 245425 (2006).
[4]V. I. Tokar and H. Dreyssé, Phys. Rev. B **74**, 115414 (2006).
[5]V. I. Tokar and H. Dreyssé, Phys. Rev. B **76**, 073402 (2007).
[6]P. Kocán, P. Sobotík, and I. Ošt'ádal, Phys. Rev. B **74**, 037401 (2006).
[7]M. A. Albao, M. M. R. Evans, J. Nogami, D. Zorn, M. S. Gordon, and J. W. Evans, Phys. Rev. B **74**, 037402 (2006).
[8]I. Ošt'ádal, J. Javorský, P. Kocán, P. Sobotík, and M. Setvín, J. Phys.: Conf. Ser. **100**, 072006 (2008).
[9]P. Kocán, P. Sobotík, I. Ošt'ádal, M. Setvín, and S. Haviar, Phys. Rev. E **80**, 061603 (2009).
[10]N. Takeuchi, Phys. Rev. B **63**, 035311 (2000).
[11]M. C. Bartelt and J. W. Evans, Phys. Rev. B **46**, 12675 (1992).
[12]J. A. Blackman and P. A. Mulheran, Phys. Rev. B **54**, 11681 (1996).
[13]P. Kocán, P. Sobotík, I. Ošt'ádal, J. Javorský, and M. Setvín, Surf. Sci. **601**, 4506 (2007).
[14]M. A. Albao, J. W. Evans, and F. Chuang, J. Phys. Condens. Matter **21**, 405002 (2009).
[15]J. G. Amar and F. Family, Phys. Rev. Lett. **74**, 2066 (1995).
[16]A. Zangwill and E. Kaxiras, Surf. Sci. **326**, L483 (1995).
[17]P. Jensen, H. Larralde, and A. Pimpinelli, Phys. Rev. B **55**, 2556 (1997).
[18]P. A. Mulheran and D. A. Robbie, Philos. Mag. Lett. **78**, 247 (1998).
[19]D. A. Robbie and P. A. Mulheran, Comput. Mater. Sci. **17**, 500 (2000).
[20]N. Zaki, D. Potapenko, P. D. Johnson, and R. M. Osgood, Phys. Rev. B **80**, 155419 (2009).
[21]O. S. Hernán, A. L. V. de Parga, J. M. Gallego, and R. Miranda, Surf. Sci. **415**, 106 (1998).
[22]F. Nouvertné, U. May, M. Bamming, A. Rampe, U. Korte, G. Güntherodt, R. Pentcheva, and M. Scheffler, Phys. Rev. B **60**, 14382 (1999).
[23]R. Miranda and J. M. Gallego, Phys. Rev. B **64**, 085426 (2001).
[24]R. Pentcheva, K. A. Fichthorn, M. Scheffler, T. Bernhard, R. Pfandzelter, and H. Winter, Phys. Rev. Lett. **90**, 076101 (2003).
[25]V. I. Tokar and H. Dreyssé, Phys. Rev. B **77**, 165424 (2008).
[26]M. B. Yilmaz and F. M. Zimmermann, Phys. Rev. E **71**, 026127 (2005).
[27]V. I. Tokar and H. Dreyssé, Phys. Rev. B **68**, 195419 (2003).
[28]V. I. Tokar and H. Dreyssé, Phys. Rev. E **68**, 011601 (2003).
[29]V. S. Stepanyuk, A. N. Baranov, D. V. Tsivlin, W. Hergert, P. Bruno, N. Knorr, M. A. Schneider, and K. Kern, Phys. Rev. B **68**, 205410 (2003).
[30]J. C. Slater, J. Chem. Phys. **41**, 3199 (1964).
[31]M. D. Morse, Chem. Rev. **86**, 1049 (1986).
[32]M. Giesen and G. S. Icking-Konert, Surf. Rev. Lett. **6**, 27 (1999).
[33]J. W. Evans, P. A. Thiel, and M. C. Bartelt, Surf. Sci. Rep. **61**, 1 (2006).
[34]D. D. Chambliss and K. E. Johnson, Phys. Rev. B **50**, 5012 (1994).
[35]F. M. Ross, J. Tersoff, and R. M. Tromp, Phys. Rev. Lett. **80**, 984 (1998).
[36]G. Medeiros-Ribeiro, A. M. Bratkovski, T. I. Kamins, D. A. A. Ohlberg, and R. S. Williams, Science **279**, 353 (1998).
[37]J. E. Prieto, J. de la Figuera, and R. Miranda, Phys. Rev. B **62**, 2126 (2000).
[38]C. Ratsch and J. A. Venables, J. Vac. Sci. Technol. A **21**, S96 (2003).
[39]V. I. Tokar and H. Dreyssé, Philos. Mag. **88**, 2747 (2008).
[40]C. Priester and M. Lannoo, Phys. Rev. Lett. **75**, 93 (1995).
[41]K. Binder, in *Monte Carlo Methods in Statistical Physics*, edited by K. Binder, Topics in Current Physics, Vol. 7 (Springer-Verlag, Heidelberg, 1986), p. 1.
[42]V. I. Tokar and H. Dreyssé, Phys. Rev. E **77**, 066705 (2008).
[43]G. Nandipati, Y. Shim, and J. G. Amar, Phys. Rev. B **81**, 235415 (2010).
[44]H. Brune, G. S. Bales, J. Jacobsen, C. Boragno, and K. Kern, Phys. Rev. B **60**, 5991 (1999).
[45]S. J. Koh and G. Ehrlich, Phys. Rev. B **62**, R10645 (2000).
[46]N. Zaki (private communication).
[47]K. Morgenstern, E. Lægsgaard, I. Stensgaard, and F. Besenbacher, Phys. Rev. Lett. **83**, 1613 (1999).
[48]I. Lifshitz and V. Slyozov, J. Phys. Chem. Solids **19**, 35 (1961).
[49]C. Wagner, Z. Elektrochem. **65**, 581 (1961).